Raman-active phonons in $La_4BaCu_5O_{13}$: polarized Raman spectroscopy and lattice dynamical calculations

1995 J. Phys.: Condens. Matter 7 4967

(http://iopscience.iop.org/0953-8984/7/25/019)

J. Phys.: Condens. Matter 7 (1995) 4967–4973. Printed in the UK

Raman-active phonons in $La_4BaCu_5O_{13}$: polarized Raman spectroscopy and lattice dynamical calculations

M V Abrashev and V N Popov
Faculty of Physics, Sofia University, BG-1126 Sofia, Bulgaria

Received 14 February 1995, in final form 3 May 1995

Abstract. Polarized Raman spectra of the perovskite-like compound $La_4BaCu_5O_{13}$ were measured and the symmetry of the observed lines was determined. A calculation of the Raman-active phonon modes ($10A_g + 10B_g + 5E_g$) within a shell model was additionally used to support the mode assignment and to obtain the ionic vibrational patterns. The observed and calculated frequencies were also compared with the available data for similar structures.

1. Introduction

$La_4BaCu_5O_{13}$ is an ordered oxygen-deficient perovskite first reported by Michel and co-workers [1]. Its structure is tetragonal, space group P4/m (C_{4h}^1), $a = 8.6475$ Å $\approx a_p\sqrt{5}$, $c = 3.8594$ Å $\approx a_p$ [2]. The La and Ba atoms are located in an ordered manner. The oxygen vacancies are ordered in chains along the c axis. The Cu_5O_{13} framework consists of corner sharing CuO_5 pyramids and CuO_6 octahedra (see figure 1). Each octahedral chain is surrounded by four pyramidal chains. An interesting feature of the structure is that each two adjacent pyramids in the ab plane are oriented perpendicular one to another, i.e. an O3 oxygen atom (see table 1) is an apex one for one of the pyramids but a basal one for the other. The oxygen absorption–desorption studies [1, 3] have shown that the oxygen stoichiometry is unusually stable in both air and oxygen atmospheres up to the synthesis temperature (≈ 1000 °C). The metastable phases $La_4BaCu_5O_{13-x}$ ($x = 0.5$, 1, 2) were obtained after annealing in He or H_2/Ar atmospheres [3]. $La_4BaCu_5O_{13}$ exhibits metallic conductivity of the same order of magnitude as that of the high-T_c superconductors in the normal state, but it is not superconducting down to 1.3 K [1, 4, 5]. Electronic structure calculations [6] suggest that the band structure near the Fermi level is 3D rather than 1D. However, no studies on monocrystals have been made up to now to verify the latter suggestion. Recently, a disordered cubic perovskite ($a = 3.877$ Å) with the same chemical content and metallic properties has been stabilized in the form of a thin film by laser ablation [7].

In this paper we present polarized Raman spectra and lattice dynamical calculations for the Raman-active phonons of $La_4BaCu_5O_{13}$. The frequencies and vibrational patterns in this structure are discussed, exploring the similarity of the environment of the atoms in this compound and similar layered cuprates.

2. Experimental

To prepare $La_4BaCu_5O_{13}$ samples the starting components (La_2O_3, $BaCO_3$ and CuO) were mixed in appropriate ratios and prefired in air at 900 °C for 15 h. The resulting material was

0953-8984/95/254967+07$19.50

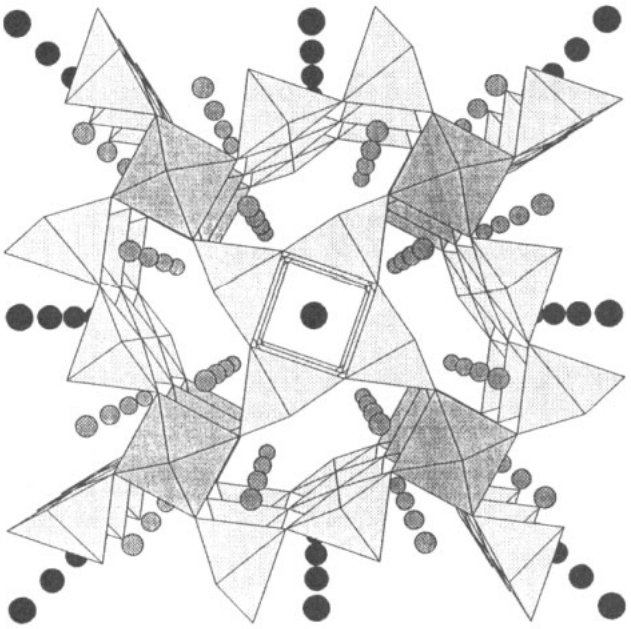

Figure 1. The structure of $La_4BaCu_5O_{13}$. The c axis is perpendicular to the sheet. The black circles are Ba atoms, the gray ones are La atoms. The copper–oxygen sublattice is presented in the form of corner-sharing octahedra and pyramids. To emphasize the chained ordering of the building units more than one unit cell ($2a \times 2b \times 3c$) is shown.

Table 1. Normal modes in $La_4BaCu_5O_{13}$.

Atom	Wickoff notation	Site symmetry	Normal modes	Remark
Ba	1d	C_{4h}	$A_u + E_u$	
La	4k	C_s	$2A_g + A_u + 2B_g + B_u + E_g + 2E_u$	
Cu1	1a	C_{4h}	$A_u + E_u$	octahedral
Cu2	4j	C_s	$2A_g + A_u + 2B_g + B_u + E_g + 2E_u$	pyramidal
O1	1b	C_{4h}	$A_u + E_u$	oct.–oct.
O3	4j	C_s	$2A_g + A_u + 2B_g + B_u + E_g + 2E_u$	pyr.–pyr. 'apex'
O4	4j	C_s	$2A_g + A_u + 2B_g + B_u + E_g + 2E_u$	oct.–pyr.
O5	4k	C_s	$2A_g + A_u + 2B_g + B_u + E_g + 2E_u$	pyr.–pyr. 'basal'

	Activity	Selection rules for the Raman-active modes	Symmetry-allowed directions of vibrations
Raman	$\mathbf{10A_g + 10B_g + 5E_g}$		
Infrared	$7A_u + 12E_u$	$A_g \rightarrow \alpha_{xx} + \alpha_{yy}, \alpha_{zz}$	in ab plane
Acoustic	$A_u + E_u$	$B_g \rightarrow \alpha_{xx} - \alpha_{yy}, \alpha_{xy}$	in ab plane
Silent	$5B_u$	$E_g \rightarrow \alpha_{xz}, \alpha_{yz}$	along c axis

ground and annealed at 950 °C for 20 h, then reground, pressed into 1 g pellets and annealed at 980 °C for 50 h. Half of the samples were rapidly quenched to room temperature. The remaining samples were slowly cooled to room temperature for 12 h.

The cell parameters as determined from the x-ray powder diffractogramms (Co Kα radiation, URD-6 powder diffractometer) are close to other published data [1–3, 8]. For

the slowly cooled samples $a = 8.650(1)$ Å, $c = 3.862(3)$ Å, and for the rapidly quenched samples $a = 8.662(3)$ Å, $c = 3.868(3)$ Å.

Careful observation of the surface of the polished sample through an optical microscope under polarized white light showed that (1) the ceramics are of single phase and consist of microcrystals of square and elongated form (depending on their orientation) with dimensions up to 80×30 μm, and (2) the microcrystals are optically anisotropic and their colour changes from white to dark yellow, for light polarized perpendicular and parallel to the c axis, respectively.

The Raman spectra were measured at room temperature using a triple multichannel spectrometer Microdil 28 (DILOR) equipped with an optical microscope. A 100× objective was used to focus the incident laser beam in a spot of about 1 μm in diameter on the surface of the microcrystals and to collect the backward-scattered light. Both 514.5 nm and 488.0 nm Ar^+ laser lines were used for excitation. To avoid overheating of the samples the laser power was kept below 2 mW.

3. Results and discussion

The classification of the normal modes in the Γ-point of the Brillouin zone is presented in table 1. The Raman-active modes belong to three symmetry species: A_g, B_g and E_g. Their corresponding Raman tensors have different nonzero components and in order to identify the Raman line symmetries it is sufficient to obtain polarized Raman spectra from two types of crystal surfaces: those containing the c axis and those perpendicular to the c axis. Microcrystals exhibiting these two types of surfaces can easily be distinguished on the polished surface of the pellet. First, the microcrystals are elongated along the c axis. Second, due to their optical anisotropy upon observation of the surface with a crossed polarizer and analyser and when the sample is rotated, the colour of the (001) surfaces remains dark whereas the colour of the ($mn0$) surfaces changes to the highest degree from dark to light every 45°. The dark colour corresponds to polarization along the c axis and in the ab plane. The polarized Raman spectra obtained from a ($mn0$) surface (containing the c axis) are presented in figure 2. In the $y(zx)\bar{y}$ spectra (using Porto's notation, z is the direction along the c axis, x and y are two arbitrary perpendicular directions in the ab plane) only E_g lines may be observed, in the $y(zz)\bar{y}$ spectra only A_g lines may be observed, and in the $y(xx)\bar{y}$ spectra A_g as well as B_g lines may be observed. A_g and B_g lines can be determined from their different appearance in the spectra obtained from a (001) surface (see figure 3; the angle between $x(y)$ and $x'(y')$ directions is 45°). The A_g lines can be observed only in parallel (xx, yy, $x'x'$ and $y'y'$) polarizations, whereas the B_g lines can be observed in parallel as well as in crossed (xy or $x'y'$) polarizations. The frequencies and symmetries of all observed lines are given in table 2.

It has already been noted that the cell parameters of the two types of sample are slightly different. The increase of the volume of the cell is connected with the decrease of its oxygen content (see [3]). In the Raman spectra of some layered cuprates (for example, Nd_2CuO_{4-y} and $YBa_2Cu_3O_{7-\delta}$) defect modes with an intensity comparable to that of the rest modes have been observed due to the oxygen nonstoichiometry. In our case the Raman spectra obtained from the two types of samples were identical. This fact gives us the confidence to state that all observed lines originate from symmetry-allowed modes. The only exception is the line at 99 cm^{-1}, which appears always in crossed polarization and does not depend on the orientation of the crystal surface. We attribute it to the Raman scattering from air.

The calculations of the lattice dynamics of $La_4BaCu_5O_{13}$ were made using a shell model [9]. This model properly accounts for the predominant ionic character of the cuprates

Table 2. Experimental and calculated frequencies (in cm^{-1}) of the Raman-active modes in $La_4BaCu_5O_{13}$.

A_g			B_g			E_g		
ν_{exp}	ν_{calc}	Atoms	ν_{exp}	ν_{calc}	Atoms	ν_{exp}	ν_{calc}	Atoms
—	531	O4	570	568	O3	575	578	O5
486	511	O3	—	491	O4	371	387	O3
478	468	O3	471	474	O5,O4,O3	306	313	O4
402	400	O5	410	398	O5	157	156	Cu2
339	337	O5,O4,O3	307	343	O5,O4,O3	—	114	La
267	271	O4	299	298	O3,O4			
235	200	Cu2,O3	223	216	Cu2,O4,O3			
—	182	La,O3,Cu2	168	188	La,O3,Cu2,O5			
155	166	Cu2,O3	144	142	Cu2			
—	64	Cu2,La	126	111	La			

describing the interionic interactions via long-range Coulomb potentials and short-range ones, here chosen to be of Born–Mayer–Buckingham form:

$$V = a\exp(-br) - \frac{c}{r^6}. \tag{3.1}$$

Here a, b and c are parameters, and r is the interionic distance. The ionic polarizability α is also included in the model considering that each ion (with charge Z) consists of a charged core surrounded by a charged shell (with charge Y). The model parameters are often transferred from other substances, whose lattice dynamics has been well studied. Such an approach reduces the ambiguity in the parameter set and leads to plausible predictions. Here the initial values of the parameters (see table 3) are taken from previous studies of a number of layered copper oxides [9]. The obtained model is stable everywhere in the Brillouin zone. In order to get better correspondence of the calculated O3 and O4 E_g modes with the observed ones, the charge Y_{O4} was altered to -2.00, while α_{O3} and α_{O4} were assumed to be anisotropic with values as large as $5.00\,\text{Å}^3$ in the c direction. It is worth mentioning that such a correction was also necessary for the apex oxygen ions in La_2CuO_4 (see for example [11]). The calculated frequencies are compared with the experimental ones in table 2. It is difficult to describe the pattern of some of the modes, especially some of the A_g and B_g ones, as more than one kind of atom vibrates and the directions of atomic displacements are rather arbitrary with respect to the crystal axes and the interatomic bonds. Therefore only the atoms participating in the modes are indicated in table 2.

Table 3. Shell model parameters for $La_4BaCu_5O_{13}$.

Ion	Z ($\|e\|$)	Y ($\|e\|$)	α (Å^3)	Ionic pair	a (eV)	b (Å^{-1})	c (eV Å^6)
La	2.85	1.70	0.7	La–O	1498	2.622	0.0
Ba	1.90	3.00	3.6	Ba–O	814	2.326	0.0
Cu	1.90	3.00	1.3	Cu–O	1500	3.553	0.0
O	−1.90	−3.00	2.0	O–O [10]	22764	6.711	20.37

Before discussing the modes, it is necessary to emphasize the similarity of the structure of $La_4BaCu_5O_{13}$ with that of $RBa_2Cu_3O_{7-\delta}$ (R = Y, rare earth), known in short as R-1237. The disposition of each two pyramids with parallel bases and an R-layer between them is

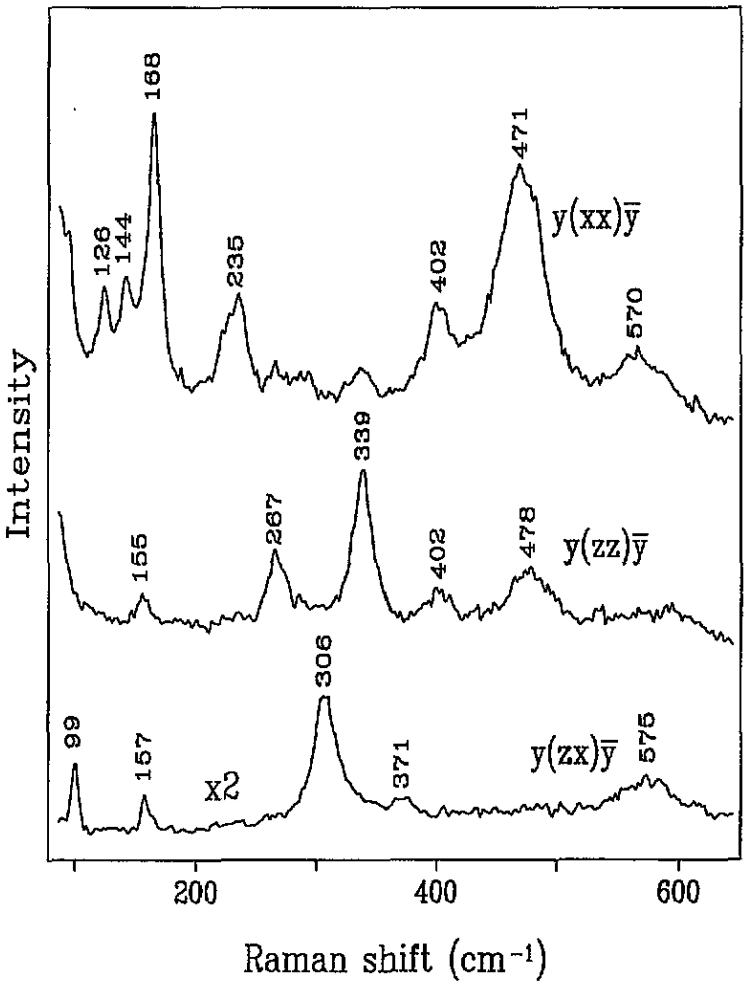

Figure 2. Polarized Raman spectra obtained from a (*mn*0) microcrystal surface (the *c* axis parallel to it). The cross polarized spectrum is multiplied by two. *x* and *y* are two arbitrary directions in the *ab* plane. $\lambda_L = 488.0$ nm.

the same as in R-1237. Thus, the modes of the O5 and Cu2 atoms will be similar to modes of O2(O3) and Cu2 atoms in R-1237. Comparing the modes of the O3 'apex' atom with their counterparts of the O4 'apex' atom in R-1237 is complicated, because in our structure the O3 atom is one of the oxygens from the base of the pyramid.

As follows from the lattice dynamical calculations, all E_g modes are pure (i.e. in each mode predominantly only one kind of atom participates). We assign the line at 575 cm^{-1} to the stretching vibration of O5 along the *c* axis. Its analogues in Y-1237 are the B_{2g} mode of O2 and the B_{3g} mode of O3 observed at 579 cm^{-1} and 526 cm^{-1}, respectively [12]. The decrease in the frequency of these vibrations correlates with the increase of the Cu–O distance. In Y-1237 the Cu2–O2 distance is 1.929 Å, in Cu2–O3 it is 1.962 Å [13], while the Cu2–O5 distance in our structure is 1.935 Å [2]. The other two high-frequency E_g lines at 371 cm^{-1} and 306 cm^{-1} are assigned to the bending vibrations along the *c* axis of O3 and O4 atoms, respectively. The closest in pattern vibration in Y-1237 is the B_{3g} mode of

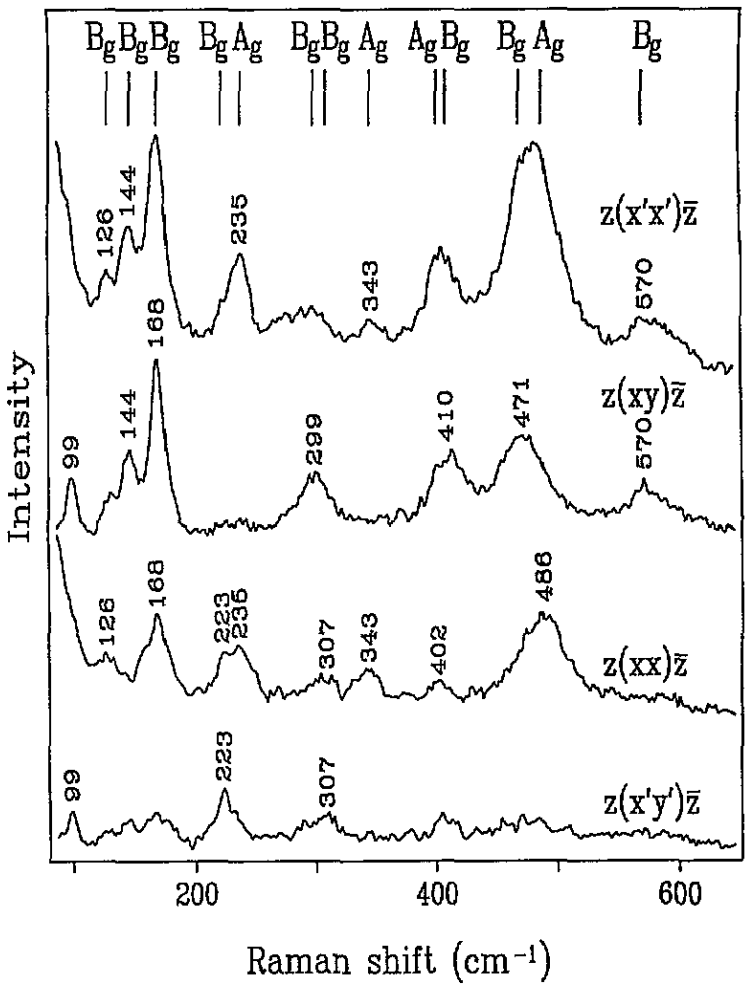

Figure 3. Polarized Raman spectra obtained from a (001) microcrystal surface. The symmetries of the lines are indicated. $\lambda_L = 488.0$ nm.

the O4 'apex' atom observed at 303 cm^{-1} [12]. Although the distances from the O3 (O4 in Y-123) to the nearest Cu atoms are very close (2.272 Å and 1.880 Å in $La_4BaCu_5O_{13}$ [2] and 2.289 Å and 1.859 Å in Y-1237 [13]) the difference between their frequencies is 68 cm^{-1}. The reason probably is the different heavy atom environment of the two 'apex' atoms: 2 La and 2 Ba for $La_4BaCu_5O_{13}$ and 4 Ba in Y-1237. The last observed E_g line at 157 cm^{-1} originates from the Cu2 vibration along the *c* axis (in the basal plane of the pyramids). The corresponding B_{2g} and B_{3g} modes of Cu2 in R-1237 have been observed at 142 cm^{-1} and 140 cm^{-1} for Y-1237 [12] and 134 cm^{-1} for Pr-1237 [14].

Some of the modes with A_g and B_g symmetry also have analogues in R-1237. We assign the A_g line at 402 cm^{-1} and the B_g line at 410 cm^{-1} to the *O5* vibration in the *ab* plane parallel to the pyramid's base. Their analogue in Pr-1237 is the B_{2g} mode of the O2 atom observed at 408 cm^{-1} [14]. Further, we assign the 155 cm^{-1} and 144 cm^{-1} lines to the A_g and B_g modes corresponding to Cu2 vibrations perpendicular to the pyramid's base. In R-1237 these modes correspond to the well studied A_g line whose frequency varies

from 140–150 cm^{-1} depending on the type of the rare earth and the oxygen stoichiometry. There are two other specific vibrations related to the four oxygen atoms in the base of the pyramid. These are the so-called 'in-phase' and 'out-of-phase' vibrations perpendicular to the pyramids' bases. In the case of R-1237 they are of A_g symmetry (A_{1g} and B_{1g} in tetragonal R-1236) and have been observed at about 440 cm^{-1} and between 297–340 cm^{-1} (varying the rare earth from La to Lu) [15]. In our case the base of each pyramid consists of two O5, one O4 and one O3 atoms. The lattice dynamical calculations show the existence of two such modes (in our case of B_g symmetry) with frequencies of 474 cm^{-1} and 343 cm^{-1}, respectively. We assign the experimentally observed 471 cm^{-1} and 307 cm^{-1} lines to these modes.

The rest A_g and B_g modes in $La_4BaCu_5O_{13}$ are specific for this structure. The calculations have given for the two high-frequency A_g (breathing for octahedral chains) and B_g (antisymmetric stretching) modes of O4 the frequencies of 531 cm^{-1} and 491 cm^{-1}, but no lines of corresponding symmetry and close frequencies have been observed in the Raman spectra. The 486 cm^{-1} (A_g), 478 cm^{-1} (A_g) and 570 cm^{-1} (B_g) lines originate from vibrations of the O3 atoms. The 267 cm^{-1} (A_g) and 299 cm^{-1} (B_g) lines can be assigned to librational modes of the octahedral and the pyramidal chains, respectively. An interesting mode with A_g symmetry (O4 and O5 in-phase, O3 out-of-phase) similar to the two mixed O3, O4, O5 bending B_g modes is represented by the 339 cm^{-1} A_g line. All the rest modes below 250 cm^{-1} (excluding the two above-mentioned Cu2 modes) are strongly mixed, and it is difficult to describe their vibrational patterns.

Acknowledgments

We thank L N Bozukov for the x-ray measurements and M N Iliev for a critical reading of the manuscript. The technical help of L Georgieva is highly appreciated. This work was supported in part by grants Nos F 410 and F 423 of the Bulgarian National Foundation for Science.

References

[1] Michel C, Er-Racho L and Raveau B 1985 *Mat. Res. Bull.* **20** 667
[2] Michel C, Er-Racho L, Hervieu M, Pannetier J and Raveau B 1987 *J. Solid State Chem.* **68** 143
[3] Davies P K and Katzan C M 1990 *J. Solid State Chem.* **88** 368
[4] Torrance J B, Tokura Y, Nazzal A and Parkin S S P 1988 *Phys. Rev. Lett.* **60** 542
[5] Tamegai T and Iye Y 1989 *Physica* **159C** 181
[6] Herman F, Kasowski R V and Hsu W Y 1988 *Phys. Rev.* B **37** 2309
[7] Desfeux R, Hamet J F, Mercey B, Simon C, Herveu M and Raveau B 1994 *Physica* **221C** 205
[8] Wong-Ng W, Kuchinski M A, McMurdie H F and Paretzkin B 1989 *Powder Diffr.* **4** 46
[9] Popov V N 1995 *J. Phys.: Condens. Matter* **7** 1625
[10] Catlow C R A, Mackrodt W C, Norgett M J and Stoneham A M 1977 *Phil. Mag.* **35** 177
[11] Mostoller M, Zhang J, Rao A M and Eklund P C 1990 *Phys. Rev.* B **41** 6488
[12] McCarty K F, Liu J Z, Shelton R N and Radousky H B 1990 *Phys. Rev.* B **41** 8792
[13] Sharma R P, Rotella F J, Jorgensen J D and Rehn L E 1991 *Physica* **174C** 409
[14] Humlicek J, Litvinchuk A P, Kress W, Lederle L, Thomsen C, Cardona M, Habermayer H U, Trofimov I E and König W 1993 *Physica* **206C** 345
[15] Rosen H J, Macfarlane R M, Engler E M, Lee V Y and Jacowitz R D 1988 *Phys. Rev.* B **38** 2460